JOURNAL OF PROPULSION AND POWER
Vol. 22, No. 3, May–June 2006

Assessment of Fission Fragments Enhancement for Nuclear Thermal Propulsion

Ivan Di Piazza* and Marco Mulas†
CRS4, 09010 Pula (Ca), Italy

A novel concept of nuclear thermal rocket (NTR) propulsion is presented. It is based on the direct conversion of the kinetic energy of the fission fragments (FFs) into the propellant enthalpy. A sufficiently large surface coated with a few micrometers of Americium 242 m, confined by a neutron diffuser, can become a critical reactor, in which the FFs can escape from the thin layer of fissionable material. The novel FF NTR propulsion concept can allow the propellant to achieve temperatures higher than the nuclear fuel, thus overcoming the limit in the specific enthalpy imposed on the propellant in the conventional solid-core NTR propulsion. A preliminary assessment of the FF NTR concept's propulsion characteristics has been carried out using an in-house developed software system that integrates a computational-fluid-dynamic code, a neutronic code and a Monte Carlo code. The assessment shows the potential to reach specific impulses of about 15,000 m/s and thrust levels in the range 4000 to 6000 N, with a thrust-to-weight ratio of a few percent of the acceleration of gravity. Such performance can make the FF propulsion a candidate for human missions to the planet Mars.

Nomenclature

B_{UP}	=	fuel burn-up
c_p	=	propellant specific heat at constant pressure
D	=	module diameter
$\mathrm{d}Q_{\mathrm{conv}}$	=	power loss of elementary volume due to heat convection
$\mathrm{d}Q_{\mathrm{gen}}$	=	power deposited inside $\mathrm{d}V$
$\mathrm{d}Q_w$	=	power loss of elementary volume due to heat conduction
$\mathrm{d}V$	=	volume of elementary module
$\mathrm{d}x$	=	small elementary portion of module length
E_F	=	engine gross nuclear energy
f	=	correction factor of order unity
h	=	average propellant stagnation enthalpy
h_w	=	average propellant stagnation enthalpy before entering heating chamber
I_{sp}	=	specific impulse
k	=	propellant thermal conductivity
k_{eff}	=	reactor multiplication factor
L	=	module length
M	=	total burnout (final) mass of spaceship
M_F	=	mass of fuel available for the mission
M_p	=	mass of propellant needed for the mission
$\dot{m}_p$	=	engine mass flow rate
$\dot{m}_w$	=	mass flow rate per unit surface
N	=	number of modules
Pe	=	Peclet number
Pr	=	Prandtl number, ν/α
p_c	=	propellant stagnation pressure
$\dot{Q}_{\mathrm{cond}}$	=	power loss due to heat conduction
$\dot{Q}_F$	=	gross nuclear fuel power
$\dot{Q}_{\mathrm{FF\_lost}}$	=	power not transferred from the FFs to the propellant
$\dot{Q}_h$	=	heating power available for generating thrust
$\dot{Q}_{\mathrm{nozzle}}$	=	power loss associated to the flow in the nozzle
$\dot{Q}_p$	=	propulsion power of the engine
$\dot{q}_{\mathrm{FF}}$	=	rate of fuel energy consumption per unit surface of fuel layer
$\dot{q}_w$	=	wall heat flux
Re	=	Reynolds number
S	=	lateral surface of the heating tube
T_{li}	=	lithium temperature
T_w	=	wall temperature
α	=	propellant thermal diffusivity
Δh	=	enthalpy increase due to the direct energy conversion process
Δh_{diss}	=	dissociation enthalpy of hydrogen
ΔV	=	velocity change
δ_F	=	thickness of fuel layer
η	=	overall efficiency
η_{capture}	=	FF capture efficiency
η_{FF}	=	fission fragments efficiency
η_h	=	heating efficiency
η_{layer}	=	Americium layer efficiency
η_N	=	nozzle efficiency
ν	=	propellant kinematic viscosity
ρ_F	=	density of fuel layer
τ_F	=	fuel duration
τ_p	=	propellant duration

Received 31 January 2005; revision received 23 June 2005; accepted for publication 15 November 2005.

*Researcher, Parco POLARIS, Group of Hydrology and Water Resources Management; currently Thermo-Fluid Dynamics Analyst, Ansaldo Nucleare, 16161 Genova, Italy.

†Senior Researcher, Parco POLARIS, Group of Computational Fluid Dynamics. Member AIAA.

Introduction

THE nuclear thermal rocket (NTR) represents a relatively mature advanced propulsion technology that can be considered for near-future human missions to Mars.[1,2] In principle, nuclear propulsion can allow much higher specific impulses, in comparison to chemical propulsion: the energy available from one unit mass of fissionable material is 10^7 times larger than that available from chemical reactions. The heat of combustion of the most energetic reaction (liquid oxygen and liquid hydrogen) limits the specific impulse I_{sp} to about 4 km/s, which corresponds to a specific enthalpy of the propellant below 10^7 J/kg. Specific enthalpies of 10^8 and 10^9 J/kg, in principle easily attainable with a nuclear energy source, would lead to specific impulses well above 10 and 30 km/s, respectively. By looking at the rocket equation (1), which limits the mission that any rocket can complete as a function of rocket specific impulse, such values can open the doors to interplanetary human space exploration:

$$M_p = M(e^{\Delta V/I_{\mathrm{sp}}} - 1) \tag{1}$$

In Eq. (1) the effects of gravity have been disregarded, and so it is only valid for propulsion systems with a high thrust-to-weight ratio.

NTR refers to conventional solid-core thermal rocket. It is based on conventional convective heat-transfer mechanism between a solid "hot" material (fissioning fuel) and a "cold" propellant. Starting in the mid-1950s, the NERVA (Nuclear Engine for Rocket Vehicle Application) NTR project[3] was developed in the United States in order to make Mars exploration by humans feasible. In the NERVA concept, the rods of a fission nuclear reactor were cooled by a hydrogen flow with a standard convective heat-transfer mechanism. To keep the fuel rods' temperature below safety limits, the engine was designed to run at very high mass flow rates of about 40 kg/s and at very high pressures, on the order of 100 bar. The overall engine weight was about 10 metric tons. A smaller version (with a mass flow rate of about 9 kg/s) was actually built and tested. When the program was terminated, ground tests showed the potential for the high mass flow rate version to reach specific impulses of about 9000 m/s and thrusts of the order of 350 kN.

The specific impulse of a conventional NTR is thus clearly limited by the need to keep the structure temperature below 3500 K, which corresponds to the hydrogen temperature between 3000 and 3500 K. This means that both NTR and chemical propulsion mechanisms operate at the same propellant temperature of the order of 3000 K, and that the superior performance of the NTR is therefore caused only by the higher specific heat of the propellant (lighter molecular weight): hydrogen vs water vapor. As a result, with respect to the space shuttle case, propellant specific enthalpies are five times larger for an NTR and the gain in the specific impulse is little more than twice as much. Though this represents an important improvement, the energy delivered to the unit mass of propellant is limited by the effect of temperature on the structure resistance and, in a sense, by the conventional heat-transfer mechanism used to convey the energy from the nuclear source.

Recently developed technological variants of NTR, such as liquid oxygen-augmented NTR, or bimodal NTR-NEP (nuclear electric propulsion)[4] do not change the potential of the baseline conventional solid-core NTR from a performance point of view.

Another concept of nuclear propulsion, based on fission reactions, is the so-called gas-core fission propulsion.[5] In such a device, the fissionable material is allowed to heat up to plasma temperatures, and its radiation is used to heat up the hydrogen gas. In this concept the propellant temperature can be significantly higher than the engine structural temperatures. The cooling of the engine walls remains however a major engineering problem.[4] This scheme can ideally reach specific impulses in the range of several tens of kilometers/second, but with a much larger weight (in the order of 100 metric tons) and a lower thrust in the range of 50 to 100 kN, and the thrust to weight ratio is lower than a solid-core NTR. Nonetheless the performance would allow shortening the total roundtrip time to Mars to less than a year[5] compared to over two-and-a-half years needed to fly on the Hohmann route,[6] the transfer ellipse that connects the orbits of Earth and Mars with minimum mission ΔV. However, the gas-core reactor represents a more far-term option, for many technological challenges have still to be solved.

Another concept that also needs a more detailed engineering design is based on heating a hydrogen flow by using a plasma fusion reactor. It represents an enhancement of a plasma fusion propulsion, where the propellant is the fuel itself (light hydrogenous ions). A preliminary engineering design[7] shows that adding a hydrogen mass flow rate of a few kilograms/second can lead to specific impulses of 1.1–1.2 km/s with a thrust of several tens of kilonewtons.

A new nuclear rocket concept has been recently introduced by Rubbia,[8] based on an idea also proposed by Ronen,[9] who showed that fuel elements of Americium 242m of less than 1 μm, with BeO as moderator, can guarantee k_{eff} large enough to have the possibility of having an actual reactor design. The fission fragments (FF) can escape from such an ultra thin layer carrying over 45% of the total fission product energy. Without discussing engineering details, Ronen proposed using the FFs to heat a gas up to a high temperature for propulsion purposes. A hydrogen mass flow enhances the fission fragments propulsion concept,[10] where the FFs, moving with a velocity of several percent of the speed of light, are the propellant working fluid.

The work presented in this paper is based on the work of Rubbia and discusses a preliminary engineering design of a fission-fragments propulsion enhancement. In this design, the FFs escaping from an ultra thin layer of few micrometers of Americium 242m are used to heat up a hydrogen flow. Heavy ionizing fragments produced by neutron-induced nuclear fission carry the major part of the corresponding fission energy in the form of kinetic energy (about 168 MeV out of 191 MeV per fission). FFs convert all of their kinetic energy into internal energy of the propellant gas, slowing down via electromagnetic interaction, provided that a sufficient thickness of propellant is present (about 500 μg/cm^2).[8] By this unconventional (direct) heat-transfer mechanism, the enthalpy of the gas in the stagnation chamber can reach values of about 200–300 MJ/kg, at low pressures of few bars, corresponding to temperatures of about 4000 to 4800 K and to a specific impulse I_{sp} of the order of 15,000–20,000 m/s. At such low pressures, compared to order 100 bar of conventional NTR, hydrogen dissociation occurs, with an associated enthalpy change of $\Delta h_{\text{diss}} = 230$ MJ/kg. This reaction contributes to store energy in the chemical bonds, rather than as sensible enthalpy, keeping the temperature lower.

Compared to the convective heat-transfer mechanism, the direct energy conversion might allow the propellant to heat up to temperatures higher than the material temperatures, thus outperforming the conventional NTR concept in terms of propellant specific enthalpies: the hydrogen flow can enter the stagnation chamber at low temperature (say in the range 1500, 2000 K) and can heat up while flowing towards the nozzle.

The objective of the this paper is to present a preliminary assessment of the thermodynamic and propulsive performance of the unconventional, FF NTR. Advantages, disadvantages, and open questions of the propulsion concept will be discussed, compared to the conventional NTR. Important scientific and technological aspects of the system, which are likely to play a very important role in the overall design process and would necessitate the interaction of many specialized scientific teams (neutronics outputs, physicochemical behavior of the Americium thin layer under thermal and mechanical stress, etc.), are either neglected or some realistic assumptions are made. The scientific feasibility of the FF unconventional NTR concept has been demonstrated in Ref. 8, and an integrated software system has been developed and used for simulating the fluid dynamic and thermal behavior of the system.[11]

The analyses have been performed on a single heating module with three-dimensional axisymmetric simulations. The system is made of a computational-fluid-dynamics (CFD) code coupled to a neutronic code and to a Monte Carlo code. The neutronic code was developed over the past two decades at CERN, the European Center of Particle Physics. For a chosen fissile material and a given layer thickness, the neutronic code constructs a database containing the FF power density (in W/m^2), the percentage of FFs escaping the fuel layer and the kinetic energy distribution of the FFs.[8] The outputs of the neutronic code are then used by the Monte Carlo code for modeling the fission fragments emission from the fuel layer and the direct energy conversion into propellant enthalpy. An experimental validation of the interaction model is still not available. The CFD code, which computes the flow inside the engine, has been fully validated for a variety of compressible flows of fluids defined by arbitrary equations of state[12]: in this case the equation of state implements chemical equilibrium conditions for hydrogen, in a wide range of temperatures and pressures, by means of look-up tables obtained with the NASA CEA (Chemical Equilibrium for Application) code.[13]

Engine Description

General Layout

The conceptual design is based on a number N of cylindrical modules (heating tubes) immersed in a bath of boiling lithium at a temperature $T_{\text{Li}} \approx 2000$ K. Figure 1 shows a schematic representation of the engine. The tubes are internally coated with a thin layer of ^{242m}Am: because of the high cross section of ^{242m}Am (one order of

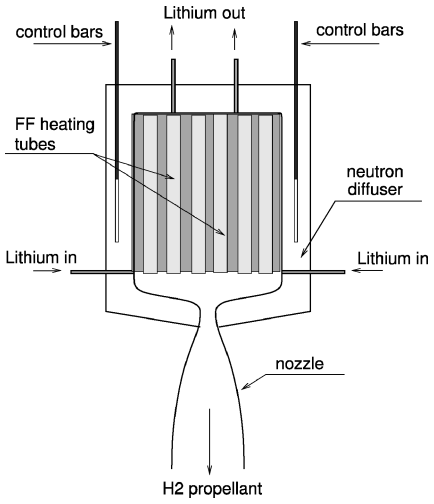

Fig. 1 Schematic representation of the FF heated propulsion engine. The configuration is a critical reactor cooled by boiling lithium and confined by a neutron diffuser. The heating chamber is made of a number of cylindrical tubes immersed in the lithium bath. Though not shown in the figure, hydrogen enters the system from the top of each heating tube as shown in next Fig. 2.

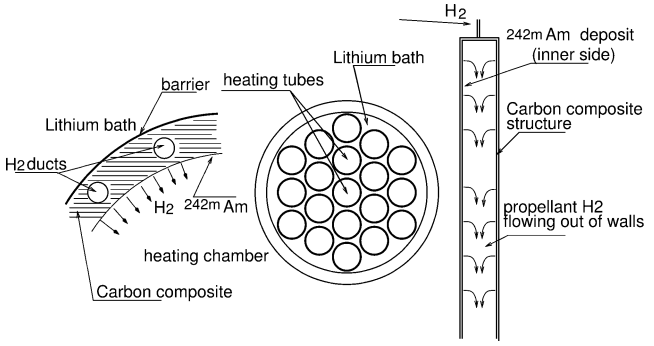

Fig. 2 Cross-section view of the heating chamber of the engine (center) with a schematic representation of the single tube (right): the cylinders are coated with the ^{242m}Am thin layer and cooled by the boiling lithium; the H_2 propellant flow enters the cylinder uniformly from the tube walls. On the left is the schematic representation of the permeable tube wall, based on the use of carbon composite fibers and matrices.

magnitude higher than that of ^{235}U), such a configuration represents a critical reactor confined by a neutron diffuser. Carbon (graphite) or beryllium (Be or BeO) can be used as reflector-moderator around the engine, and a sort of n-hohlraum can be created, assuring a multiplication factor k_{eff} sufficiently high to give a reasonable burn-up, even for a fissile layer of few micrometers of thickness. Hydrogen enters the tubes uniformly, permeating the solid walls, and heats up as it flows out of the heating tubes by absorbing the kinetic energy of the FFs.

Figure 2 shows the so-called Catiuscia arrangement of heating tubes. The tubes are constructed from carbon composite fibers and matrices, a material that is porous and permeable to hydrogen. A slab with thickness of the order of 1–2 cm with a limited number of narrow, hollow channels in which hydrogen can be introduced under pressure can provide the necessary mass flow rate of propellant $\dot{m}_p$. Preliminary simulations of the hydrogen flow through the porous material showed a pressure drop of about 40 atmo for a mass flow rate of about 4 g/s in a single heating tube. The simulations were carried out using a finite element model[14] for the Darcy law with a porosity of 0.1. The computer model also included the evaluation of the structural stresses under the thermal and mechanical loads.

The thermal and fluid-dynamic conditions of the propellant flowing inside the heating tubes depend on the volumetric heat addition coming from the FFs: the energy deposition rate, proportional to the local propellant density, heats up the propellant and so changes its temperature and density, modifying in turn the FF energy deposition rate itself. The final state of the propellant flow exiting the tubes, as well as the thermodynamic state in terms of temperature and pressure, comes from the equilibrium among many different effects: the conservation equations of mass, momentum, and energy including a model for the FF heating[8] and the H_2 dissociation. Once the fluid has been heated, it flows in the stagnation chamber, and then it is accelerated through a conventional convergent-divergent nozzle, where the internal energy is converted into kinetic energy generating thrust. The portion of nuclear fission energy that is not converted into propellant enthalpy must be evacuated by the lithium refrigerant that flows out of the core region through small tubes to the radiating panels. In a preliminary conception of the cooling system, the lithium would enter the system in liquid phase and would partially vaporize, evacuating heat from the heating tubes. The lithium returns to the liquid phase inside the radiative panels.

Because the engine has to be assembled in the International Space Station and can only be ignited in space, the number of modules that can be assembled together is limited by the size of the engine, which in turn is limited by the size of the cargo bay of the next-generation space shuttle. As an estimate, consider the dimensions of the actual space shuttle cargo bay, which is about 4.5 m in diameter and 18 m long. With the constraint of $D = 4$ m, three multiple-module arrangements are shown in Fig 3. The three configurations would fit 37, 19, and 7 modules, respectively, with diameter 0.4, 0.6, and 1 m. A perspective view of the assembled Catiuscia engine is shown in Fig. 4, where the length of the modules has been fixed to 5 m.

The following numerical values are assigned to a few variables that play an important role in understanding the concept feasibility and in quantifying the engine performance (taken from Rubbia[8]): $B_{\text{UP}} = 500$ MWday/kg (4.32×10^{13} J/kg in S.I. units), $\delta_F = 3 \times 10^{-6}$ m, $\rho_F = 13,670$ kg/m^3, and $\dot{q}_{\text{FF}} = 4$ MW/m^2. With regard to the physical-chemical form of the fuel layer, for instance, because metallic Americium melts at 1270 K, Americium carbide

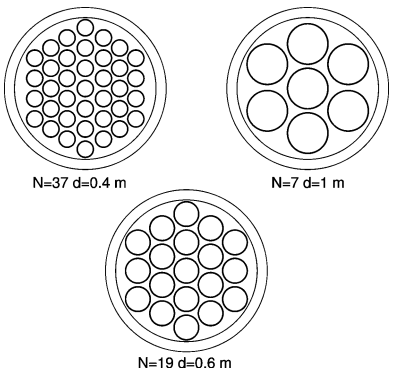

Fig. 3 Three possible Catiuscia configurations with an external diameter of 4 m. $N = 37$, 19, or 7 respectively for modules of diamater $D = 0.4$, 0.6, or 1.0 m.

Fig. 4 Perspective view of the assembled Catiuscia engine. All modules discharge in the same nozzle.

represents a potential alternative. At this stage of the development however, all values refer to metallic Americium.

Engine Overall Efficiency

The number of fissions that occurs in the engine per unit time and per unit surface of the fuel layer determines the rate at which energy is transferred to the propellant. The overall rocket engine efficiency η is defined as the ratio between the propulsion power $\dot{Q}_p$ and the gross nuclear power available from the fission process $\dot{Q}_F$:

$$\eta = \frac{\dot{Q}_p}{\dot{Q}_F} = \frac{\dot{m}_p I_{\mathrm{sp}}^2/2}{N S \dot{q}_{\mathrm{FF}}} \tag{2}$$

The propulsion power is given by

$$\dot{Q}_p = \dot{Q}_h - \dot{Q}_{\mathrm{nozzle}} = \dot{m}_p \Delta h - \dot{Q}_{\mathrm{nozzle}} = \eta_N \, \dot{Q}_h \tag{3}$$

where $\dot{Q}_{\mathrm{nozzle}}$ represents the losses associated with the expansion process in the converging-diverging supersonic nozzle caused by the missed chemical recombination into molecular hydrogen and eventually the frictional and heat flow losses at the nozzle walls. In Eq. (3) the nozzle efficency $\eta_N < 1$ has been introduced. The gross fission fragment power $\dot{Q}_F$ is converted into heating stagnation power $\dot{Q}_h$ with several losses. This power budget can be expressed as

$$\dot{Q}_h = \dot{Q}_F - \dot{Q}_{\mathrm{FF\_lost}} - \dot{Q}_{\mathrm{cond}} \tag{4}$$

where $\dot{Q}_{\mathrm{FF\_lost}}$ represents the power associated with the fission fragments that remain entrapped in the fuel layer and in the tube structure or escape from the system, never becoming available for heating the propellant; the third term $\dot{Q}_{\mathrm{cond}}$ represents the power loss as a result of heat conduction through the tubes' walls. The Reynolds number associated with the flow inside the heating tubes might, in fact, be low enough so that heat-conduction losses can be important. The two sources of power that are lost return to the tube structure and need be evacuated by the lithium refrigerant through the radiative panels. By introducing two more efficiencies η_{FF}, that takes into account the FF losses and η_h for the heat-transfer losses, the heating power $\dot{Q}_h$, representing the power that remains available for conversion into propulsive power, is given by

$$\dot{Q}_h = (\eta_{\mathrm{FF}} \eta_h) \dot{Q}_F \tag{5}$$

or, by introducing $\eta_{\mathrm{FF}} = \eta_{\mathrm{layer}} \eta_{\mathrm{capture}}$:

$$\dot{Q}_h = (\eta_{\mathrm{layer}} \eta_{\mathrm{capture}} \eta_h) \dot{Q}_F \tag{6}$$

where the FF losses have been split into two contributions: one, η_{layer}, caused by the FFs, which leave part or all of their power inside the fuel layer (FFs that cannot escape from the thin layer, for instance), and the second one, η_{capture}, caused by insufficient gas thickness present inside the tube to stop all available FFs escaping from the fuel layer. By combining all relations, an expression for the overall engine efficiency η is given by

$$\dot{Q}_p = (\eta_{\mathrm{layer}} \eta_{\mathrm{capture}} \eta_h \eta_N) \dot{Q}_F = \eta \dot{Q}_F \tag{7}$$

Now, η_{layer} depends on the fuel thickness (the thinner the layer, the higher η_{layer}), on the fuel chemical form (metallic rather than carbide, for instance) as well as on neutronic issues, and it is always less than 0.5 for symmetry reasons (half of the FFs would tend to escape from the wrong side, converting their energy into heat of the wall structure). Neutronic simulations[8] provided a value for the layer efficiency given by $\eta_{\mathrm{layer}} = 0.31$, which means that 70% of the overall power $\dot{Q}_F$ is instantaneously converted into heat.

The second efficiency η_{capture} measures the amount of power extracted by the FFs during the interaction with the flowing propellant and depends upon the gas thickness and on the propellant thermodynamic pressure as a consequence. Its actual value depends on the design choices in terms of operating pressure and nozzle throat area: the higher the pressure, the higher η_{capture} (eventually approaching unity), but the smaller the throat area increases the nozzle losses caused by heat transfer. Values obtained in the simulations carried out are in the range between 0.75 and 0.95.

Table 1 Efficiencies of the FF NTR concept

Efficiency	Value
η_{layer}	0.3
η_{capture}	0.7–0.95
η_h	0–1
η_N	0.6

FFs that remain entrapped in the structure can cause material damage and structural swelling because of further FF decay. These issues have not been studied and might need further investigation.

The third efficiency, called the heating efficiency, measures the power loss caused by the heat conduction through the tube walls. The heating efficiency is the crucial efficiency, for it can vary widely, depending on the operating conditions. High mass flow rates (high Reynolds numbers) will allow a high η_h, a low propellant specific enthalpy, and a low specific impulse. In contrast, high specific impulses and low efficiencies will be obtained running the engine at low mass flow rates because of increased conductive losses.

Finally η_N is the nozzle efficiency. The value of $\eta_N \approx 0.60$ represents a good approximation if the accelerating flow inside the nozzle remains in chemical equilibrium conditions and if negligible viscous and wall heat-transfer losses occur. This will turn out to be a good approximation if the nozzle dimensions are not too small. (Again, a high nozzle Reynolds number results in negligible heat-transfer losses: the nozzle throat area does not have to be too small.) Again, the design pressure in the stagnation modules appears as one of the critical design choices for the whole system. The lowest possible pressure seems to be the optimal choice, provided that η_{capture} remains at an acceptable level.

A summary of all efficiencies is given in the Table 1 for the sake of clarity. By considering the values just discussed, the overall engine efficiency η is smaller than about 0.16. The power losses associated with (η_{layer} η_{capture} η_h) represent the heat that must be removed by cooling the external walls by the lithium loop and by the radiative panels. If $\eta_h \approx 1$, such a power loss amounts to the 74% (minimum) of the gross nuclear power. The remaining 10% of the initial power is associated with the nozzle efficiency and represents mostly the power stored in the chemical bonds of atomic hydrogen (missed recombination of molecular hydrogen in chemical equilibrium conditions). This portion is is directly lost to deep space. The lower η_h, with respect to unity, the higher the power percentage that must be evacuated through the lithium loop, which must then be designed for evacuating all of the power, as in the case of zero-propellant mass flow rate with the nuclear reactor operating at 100% power.

In the next section a correlation for the heating efficiency η_h is given, based on one-dimensional approximation.

Approximate Analytical Model of the Single Module

One-Dimensional Approximation

This model is based on the mass and power balances of the single heating module[15] shown schematically in Fig. 5.

The walls are kept at a constant temperature T_w, and thus the propellant will be preheated while permeating the solid walls of the carbon-carbon structure and will enter the heating tube with the inlet enthalpy h_w. The heating process by the FFs can be approximately described by a constant power per unit volume $\dot{Q}$ (units W/m^3), given by

$$\dot{Q} = \frac{\dot{q}_{\mathrm{FF}} \eta_{\mathrm{FF}} S}{\pi D^2/4L} \tag{8}$$

The mass flow rate is provided from the solid wall at a constant specific rate per unit area $\dot{m}_w$ (kg/m^{2}s). If an x-coordinate system is defined along the module axis, mass and energy balances can be made with reference to an infinitesimal portion dx of the module

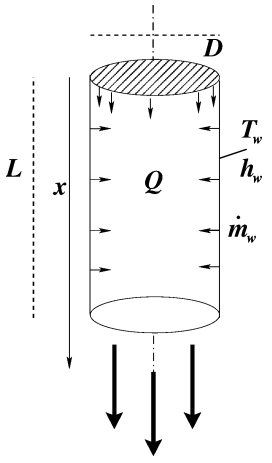

Fig. 5 Schematic representation of the heating module.

of volume $dV = \pi(D^2/4)\,dx$. The balances refer to sections located far from the top of the module, in which an asymptotic radial temperature profile, and thus an asymptotic section-average enthalpy level has been reached.

It can be shown that the mass flow rate at the exit section located at L is

$$\dot{m}(L) \approx \dot{m}_w \pi D L \tag{9}$$

The energy balance can be written in the following way:

$$dQ_{\text{gen}} = dQ_{\text{conv}} + dQ_w \tag{10}$$

where dQ_{gen} is the power deposited in the volume dV, while dQ_{conv} and dQ_w represent the power extracted by convection and the power loss for heat conduction at the walls. The three pieces of Eq. (10) can now be estimated separately. The power generation in the volume dV is

$$dQ_{\text{gen}} = \dot{Q}\pi(D^2/4)\,dx \tag{11}$$

If $h(x)$ is the average gas enthalpy at section x, by introducing the new variable $\Delta h(x) = h(x) - h_w$, the power extracted by convection in the volume dV can be computed as

$$dQ_{\text{conv}} \approx \Delta h(x)\dot{m}_w \pi D\,dx \tag{12}$$

For relatively low Reynolds numbers and with internal heat generation, the temperature profile maintains the parabolic shape of the pure conductive case. The wall heat flux $\dot{q}_w$ can then be expressed as

$$\dot{q}_w = f\tfrac{16}{3}(k\Delta h/c_p D) \tag{13}$$

where a correction factor $f > 1$ has been introduced to account for the higher FF power deposition close to the walls caused by the higher hydrogen density. The CFD calculations showed that a correction factor $f \approx 1.5$ is appropriate.

From this relation, the total power exiting from the side walls in the volume dV can then be written as

$$dQ_w = \dot{q}_w \pi D\,dx = \tfrac{16}{3} f\pi(k/c_p)\Delta h\,dx \tag{14}$$

With the terms 11, 12, and 14 explicitly written, the power balance 10 can be revisited. The enthalpy drop can thus be finally expressed as:

$$\Delta h = \frac{\dot{Q}D^2/4}{\dot{m}_w D + (16/3) f(k/c_p)} \tag{15}$$

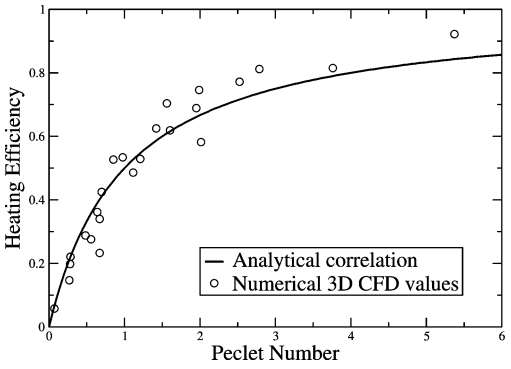

Fig. 6 Comparison between analytical correlation for heating efficiency and three-dimensional numerical simulations.

Correlation for the Heating Efficiency

The heating efficiency η_h can be derived from the main result of the analytical one-dimensional model of Eq. (15). In fact, the heating efficiency is defined as

$$\eta_h = \frac{\dot{m}(L)\Delta h}{\pi D L \eta_{\text{FF}} \dot{q}_{\text{FF}}} \tag{16}$$

By introducing the expressions derived for $\dot{m}(L)$, Δh, and $\dot{Q}$ in Eq. (16), it is possible to express the heating efficiency in the following way:

$$\eta_h = Pe/(1 + Pe) \tag{17}$$

where Pe is the tube Peclet number defined as

$$Pe = \tfrac{3}{16} 1/(\rho\alpha f)\dot{m}_w D \tag{18}$$

The Peclet number represents the product of the Prandtl number and a particular form of a Reynolds number given by

$$Re = \tfrac{3}{16} 1/(\rho\nu f)\dot{m}_w D \tag{19}$$

where all of the physical properties are to be evaluated at a constant average temperature. A comparison between the correlation of Eq. (17) and the heating efficiencies computed with CFD calculations shown in Fig. 6 shows an excellent agreement.

Performance Assessment

FF Engine Optimization

The choice of interplanetary mission and the route determines the necessary ΔV. Consider, for example, a mission between Earth and Mars. The cheapest way to get to Mars is on the Hohmann transfer. A round trip from the low Earth orbit (LEO) of the International Space Station to a low Mars orbit (LMO) would require a velocity change of about $\Delta V = 23{,}000$ m/s. If, in 20 or 30 years from now, humans will routinely travel to Mars, it is reasonable to think of starting from a LEO coplanar to the ecliptic: moving the International Space Station orbit from today's 51 to 23 deg will reduce the overall velocity change from LEO to LMO and back, on a Hohmann transfer, to about $\Delta V = 11{,}500$ m/s.

For the sake of simplicity, without entering into the mission design business, one can think of mission requirements of, for instance, 12 and 6 km/s: the first one can represent either a round-trip requirement on a Hohmann transfer, or a one-way trip on a faster route (inbound or outbound); the second one can represent a one-way trip on a Hohmann transfer. One approach could be that of having light spaceships, with crew onboard, running on faster than Hohmann transfers and using FF propulsion. Whereas one-way unmanned heavy cargo missions on Hohmann transfer can be utilized to bring all that would be needed to land on the planet to stay the required time and also to bring the return spaceship for the crew to get back to the Earth. For the unmanned cargo missions, conventional NTR or nonnuclear propulsion systems could be used. What matters is that the manned trips should move the crew quickly and safely.

Table 2 Examples of FF engine configurations

D, m	N	M_F, kg	$\dot{Q}_F$, MW	$\dot{q}_{\rm FF}$, MW/m^2	τ_F, days	L, m
0.4	37	4.8	230	2	8	2.5
0.6	19	3.7	179	2	8	2.5
1.0	7	2.3	110	2	8	2.5
1.0	7	2.3	220	4	4	2.5
1.0	7	4.6	220	2	8	5.0
1.0	7	9.2	440	4	4	5.0

One important concern is the availability of the nuclear fuel: there must be enough nuclear fuel M_F for accomplishing the mission, and the nuclear reactor must be able to keep at criticality at the full nominal power for a time interval at least equal to the time needed to consume all of the propellant at the nominal mass-flow rate.

The time τ_F needed to exhaust the nuclear fuel to below criticality is given by the ratio of the engine gross energy E_F to the engine gross power $\dot{Q}_F$:

$$E_F = M_F B_{\rm UP} = NS\delta_F \rho_F B_{\rm UP} \tag{20}$$

$$\dot{Q}_F = NS\dot{q}_{\rm FF} \tag{21}$$

Because both terms scale with the total surface area NS, τ_F does not depend on the number of modules, nor on their diameter.

$$\tau_F = E_F/\dot{Q}_F = \delta_F \rho_F B_{\rm UP}/\dot{q}_{\rm FF} \tag{22}$$

The time τ_F represents the engine maximum duration, depends only on the layer thickness and on neutronic and nuclear criticality issues, and it is inversely proportional to the rate of fuel consumption.

On the other hand, the time τ_P needed to consume all of the propellant mass M_P is simply given by the ratio of M_P to the propellant mass-flow rate $\dot{m}_p$. By using the rocket equation (1),

$$\tau_P = M_p/\dot{m}_p = M(e^{\Delta V/I_{\rm sp}} - 1)/\dot{m}_p \tag{23}$$

Without resorting to refueling options, the mission is possible if the engine maximum duration τ_F is greater than the propellant time τ_P:

$$\tau_F > \tau_P \tag{24}$$

or

$$\Delta V < I_{\rm sp}\, \ell_n[(\dot{m}_p \tau_F/M) + 1] \equiv \Delta V_{\rm limit} \tag{25}$$

which means that the achieveble ΔV might be limited by fuel shortage rather than by weight or propellant issues, though refueling might represent a technical option.

Table 2 shows the engine overall power, fuel mass and time of fuel duration τ_F, for various engine configurations in terms of number of modules and their diameter, length of the modules, and the rate of fuel consumption $\dot{q}_{\rm FF}$.

Figure 7 shows a schematic representation of the optimization process: starting from the mission requirements, a number of design choices have to be optimized in order to make the mission possible. The number of modules, their diameter, the overall propellant mass flow rate, and the type and quantity of the nuclear fuel determine the engine overall efficiency, the specific impulse, and the fuel burn-up such that there will be enough fuel and enough propellant to complete the mission. Engine power, weight, and thrust also represent results of the optimization procedure.

Running the engine at low efficiencies risks running out of nuclear fuel. On the other hand, the overall efficiency can be increased paying a price in terms of lower specific impulse. In other words there is a tradeoff between efficiency and specific impulse. The pressure established inside the heating tubes has an influence on the $\eta_{\rm capture}$ (the higher the pressure, the better the efficiency) and also on the throat area and on the nozzle efficiency as a consequence (the lower the pressure, the larger the nozzle and its Reynolds number, and so the higher η_N and the overall efficiency).

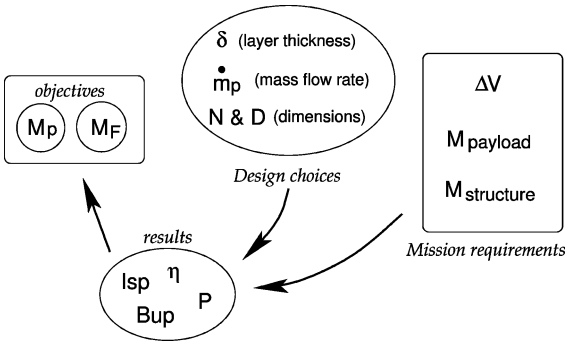

Fig. 7 Schematic representation of the optimization process for the FF rocket engine.

The criticality of the system must also be ensured[16]: clearly the reactor multiplication factor $k_{\rm eff}$ increases by increasing the overall fuel mass M_F, using more modules of smaller diameter, and with a higher operating pressure in order to keep $\eta_{\rm capture}$ high. The engine must provide a sufficiently high reactivity reserve to accomplish the mission; in other words, the burn-up must be as high as possible. A higher burn-up can be obtained increasing the thickness of the fuel layer, which in turn decreases $\eta_{\rm layer}$ together with the overall engine efficiency. The engine weight depends on the surface area of the radiative panels, which scales with the engine power, and on the size (weight) of the neutron diffuser, which depends on the multiplication factor $k_{\rm eff}$. Last but not least, the engine length (the length of the modules) has an influence on the overal power and on the $k_{\rm eff}$.

From the point of view of tube dimensions, an engine configuration with many small tubes needs a higher pressure and can determine a lower efficiency (though however increases the $k_{\rm eff}$ and the burn-up). The reverse is true for an engine configuration made of few large tubes. A global engine optimization is a problem whose solution is beyond the objectives of the present preliminary performance assessment. The understanding of how the optimization problem has to be set will however provide the guidelines for a preliminary parametric analysis of the engine performance.

Results and Discussion

A parametric analysis of the engine performance has been carried out. The analyses have been performed on a single heating module with three-dimensional axisymmetric simulations using a hybrid integrated software system[11] that integrates a CFD code and a Monte Carlo code. The latter code models the FFs trajectories into the hydrogen flow and the direct energy conversion. The focus of the analysis was on the simulation of the heating process, without considering the supersonic expansion in the converging-diverging nozzle. Inputs to the system are a database containing the FF power density (in W/m^2), the percentage of FFs escaping the fuel layer, and the kinetic energy distribution of the FFs.

The results can be expressed in terms of pressure and temperature fields, average enthalpy level of the propellant h, and efficiencies $\eta_{\rm layer}$, $\eta_{\rm capture}$, η_h. The nozzle efficiency η_N has been estimated with the NASA open source code CEA,[13] and a value of $\eta_N = 0.60$ has been assumed in the study. Three-dimensional complete simulations[17] of the whole engine have shown the basic consistency of this assumption. Once the nozzle efficiency is known, the specific impulse $I_{\rm sp}$ can be easily derived from the enthalpy h of the gas in the stagnation chamber. Each engine configuration listed in the Table 2 has been calculated for three different mass-flow rates. It can be shown via nondimensional analysis that, in the proximity of the planets, buoyant forces are negligible with respect to inertial forces, and thus buoyancy has not been considered in the numerical simulations. During the trip, in microgravity conditions, buoyant forces are absent. On the other hand, the maximum acceleration is limited by the system's thrust-to-weight ratio, which is, as it will seen later on in this paragraph, only a few percent of g_0, the acceleration of gravity at the Earth surface.

Table 3 Performance of FF engine

D, m	$\dot{q}_{FF}$, MW/m^2	$\dot{m}$, g/s	η, %	I_{sp}, km/s	$\mathcal{T}$, N	ΔV, km/s
0.4	2	19	0.91	14.8	280	3.5
0.4	2	74	3,51	14.8	1100	10.7
0.4	2	222	8.63	13.4	3000	19.2
0.6	2	38	2.96	16.7	640	7.3
0.6	2	95	6.62	15.8	1500	13.6
0.6	2	210	11.44	14.0	2950	19.5
1.0	2	35	5.26	18.2	640	7.4
1.0	2	63	8.52	17.3	1100	11.1
1.0	2	132	12.95	14.7	1950	15.6
1.0	4	105	8.72	19.1	2000	10.7
1.0	4	197	13.17	17.1	3400	15.1
1.0	4	280	15.32	15.5	4300	17.1

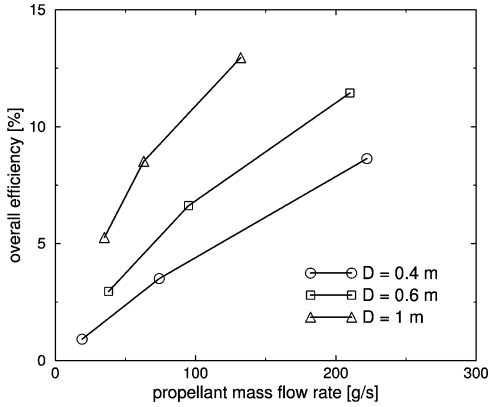

Fig. 8 Overall efficiency vs the engine mass-flow rate.

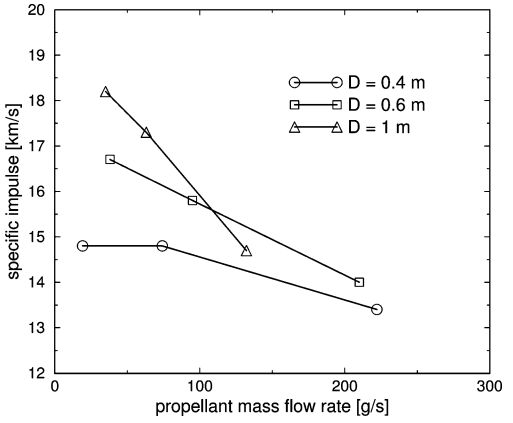

Fig. 9 Specific impulse vs the engine mass-flow rate.

Figures 8 and 9 show the results in terms of overall efficiency and specific impulse respectively vs the engine mass-flow rate. For all configurations, at the low mass-flow-rate regime the specific impulse is maximum and the efficiency minimum. At the high mass-flow-rate regime there is the tendency to approach the maximum possible overall engine efficiency of about 15–16% (zero conductive losses at high tube Reynolds numbers, and $\eta_h = 1$). The quantitative results are shown in the Table 3. All results refer to 2.5-m long modules and to a rate of fuel consumption of 2MW/m^2, except the last group which has double the rate of consumption. The last column shows the attainable velocity change before exhausting the fuel, for a total mass of the spaceship at the end of the mission of of 50 metric tons. The mission velocity drop has been calculated using the simplified version of the rocket equation, which disregards the gravity terms. A higher effective mission velocity drop has to be considered for a propulsion system with low thrust-to-weight ratio.

As shown in Table 2, doubling the rate of fuel consumption $\dot{q}_{FF}$, for the 1-m-diam configuration, results in doubling the overall engine gross power from 110 to 220 MW, and halving the time of fuel duration τ_F, which has an influence on the maximum velocity change achievable (the engine runs out of fuel in half of the time). However, the overall efficiency improves.

Note that the limit in the achievable velocity change refers to exhausting the fissile fuel and is unrelated to exhausting the propellant. By finding efficient and reliable engineering solutions to refueling, the ΔV limit would be eliminated. Nevertheless, many of the achievable velocity changes listed in the table are well above 12 km/s, which was taken as a reference value for representing a requirement for a one-way trip on a faster than Hohmann transfer route.

The slow reaction configuration with 37 modules and 40 cm diam is equivalent, from gross power point of view, to the fast reaction configuration with seven modules and 100 cm diam. Doubling the module length, to 5 ms, also would result in doubling the gross power, in this case however by paying a price in terms of a heavier spaceship, but with the same time τ_F. A 5-m-long version with the fast rate of consumption (4MW/m^2), for the seven-tube and $D = 1$ m arrangement, and a mass-flow rate of the order 600 g/s, would have a gross power of 440 MW, a specific impulse above 15,000 m/s, and a thrust in the vicinity of 10,000 N.

Operating pressures for the three diameter choices are in the range 1.5 to 3 bars, for the larger and smaller diameters respectively. Average propellant stagnation temperatures, before expansion in the supersonic nozzle, would be in the range 4000 to 4800 K, respectively for specific impulses in the range 15,000 to 18,000 m/s, and would depend also on the operating pressure (the lower the pressure, the higher the dissociation level and the lower the average temperature).

In addition, as the diameter D diminishes, the neutronic efficiency of the system increases, and thus the reactivity reserve (i.e., the burn-up) to accomplish the mission increases. Because there exist a technological burn-up limit of about 30%, the best diameter would probably be the one that guarantees this technological burn-up. From the point of view of the residual power to bring out of the system, a fixed reactivity reserve can be reached much more efficiently with smaller diameters. Concerning the weight of the spaceship, the larger the diameters of the heating tubes, the larger the moderator (Beryllium) structural mass, because of the lower multiplication factor k_{eff}. Preliminary estimations indicate that the beryllium mass can grow from 20 to 60 tons switching from the 60-cm to the 100-cm tube configuration. From these considerations, it appears that, from a neutronic point of view, small diameters would be favored, which seems in contrast with the results of Table 3. Finally, preliminary design of the lithium cooling system shows that two "sails" of approximately 13×6m^2 would be needed to evacuate 100-MW power, with an overall mass smaller than 1 ton. These figures show an approximate thrust-to-weight ratio of the FF nuclear propulsion system similar to that of the gas-core nuclear reactor: a few percent of g_0, where g_0 represents the acceleration of gravity at the Earth surface. As for the conventional NTR, a liquid-oxygen augmentation would represent a potential system for increasing the thrust, at the expenses of decreasing the specific impulse. Further optimization studies will be needed to take into account the many variables.

Conclusions

The novel concept of fission-fragments (FF) enhancement for nuclear propulsion has been described and discussed. As opposed to conventional solid-core nuclear-thermal-rocket (NTR) propulsion, which relies on the convective heat-transfer mechanism to convey the energy from the nuclear source to the propellant, the FF NTR is based on the direct conversion of the fission-fragments kinetic energy into propellant enthalpy.

A preliminary assessment of the propulsion characteristics has been discussed. The potential to reach specific impulses above 15,000 m/s has been shown. Though based only on theoretical assumptions and on computer simulation, this result represents an important improvement with respect to conventional NTR specific impulse of about 9000 m/s.

The FF rocket concept can have operating conditions, in terms of mass flow rate, thrust, and specific impulse, tailored to specific mission requirements. Another difference between FF in comparison with chemical and conventional NTR propulsion is that the achievable velocity change might be limited as a result of fuel shortage rather than to propellant shortage.

The main disadvantages, with respect to conventional NTR, are the low overall efficiency, below 16%, the lower thrust-to-weight ratio caused by the mass of the neutron diffuser, and the larger size caused by the radiative panels.

A number of key issues must still be investigated with wind-tunnel experiments and more and extensive computer simulation. The chemical form of the fuel has to be devised, and the physico-chemical behavior of the fuel layer has to be studied and tested under realistic conditions in a nuclear reactor. More studies and experiments must be devoted for assessing the effective nozzle efficiency, which was assumed equal to 0.6 throughout the paper. A further decrease of the nozzle efficiency, caused by wall heat flux, can put the whole concept in jeopardy.

Finally, finding engineering solutions for refueling during the mission would represent a major step forward for demonstrating the feasibility of the novel rocket propulsion concept for allowing human missions to the planet Mars.

Acknowledgments

This work was part of a project called P242 (identifying the isotope ^{242m} Am selected as the nuclear fuel), which was financially supported by Agenzia Spaziale Italiana.

The authors are deeply indebted to Carlo Rubbia, to his suggestions and supervision, as well as to his own actual contribution to the work. The authors wish also to thank L. Cinotti of the Nuclear Division of Ansaldo Energia for the many discussions and for the preliminary data on the moderator and on the lithium refrigeration.

References

[1]De Luca, L. T. Sackheim, R. L., and Palaszewski, B. A. (eds.), "In-Space Propulsion," *Book of Proceedings*, IWCP Vol. 10, Grafiche GSS, Bergamo, Italy, 2005.

[2]Grey, J., "Nuclear Propulsion and Power for Space: a Roundtable Discussion," *Aerospace America*, AIAA, Reston, VA, Nov. 2004, pp. 26–39.

[3]Borowski, S. K., "Nuclear Thermal Rockets: Next Step to Space," *Aerospace America*, AIAA, Reston, VA, June 1989, pp. 16–29.

[4]Frisbee, R. H., "Advanced Space Propulsion for the 21st Century," *Journal of Propulsion and Power*, Vol. 19, No. 6, 2003, pp. 1129–1154.

[5]Howe, S. D., DeVolder, B., Thode, L., and Zerkle, D., "Reducing the Risk to Mars: the Gas-Core Nuclear Rocket," *Proceedings of the Space Technology and Applications International Forum (STAIF)*, Los Alamos National Lab., Albuquerque, NM, Rept. LAUR-97-3361, Jan. 1998.

[6]Zarpette, G., Musser, G., and Alpert, M., "Special Report: Sending Astronauts to Mars," *Scientific American*, Scientific American Inc., New York, March 2000, pp. 24–33.

[7]Kammash, T., and Lee, M. J., "High-Thrust High-Specific Impulse Gas-dynamic Fusion Propulsion System," *Journal of Propulsion and Power*, Vol. 13, No. 3, 1997, pp. 421–427.

[8]Rubbia, C., "Fission Fragments Heating for Space Propulsion," CERN SL-Note 2000-036 EET, CERN, Geneva, April 2000.

[9]Chapline, G., "Fission Fragment Rocket Concept," *Nuclear Instruments and Methods A*, Vol. 271, 1988, pp. 207, 208.

[10]Ronen, Y., and Shwageraus, E., "Ultra Thin ^{242m} Am Fuel Elements in Nuclear Reactors," *Nuclear Instruments and Methods A*, Vol. 455, 2000, pp. 442–451.

[11]Mulas, M., Di Piazza, I., Pili, P., and Varone, A., "Simulation of High Enthalpy Flows Directly Heated by the Kinetic Energy of Fission Fragments," CRS4 Rept., April 2002.

[12]Mulas, M., Chibbaro, S., Delussu, G., Di Piazza, I., and Talice, M., "Efficient Parallel Computations of Flows of Arbitrary Fluid for All Regimes of Reynolds, Mach and Grashof Numbers," *International Journal of Numerical Methods for Heat and Fluid Flow*, Vol. 12, No. 6, 2002, pp. 637–657.

[13]McBride, B. J., and Gordon, S., "Computer Program for Calculation of Complex Chemical Equilibrium Compositions and Applications," NASA RP-1311, Oct. 1994.

[14]Massidda, L., and Fotia, G. M., "Progetto 242: Sviluppo di un Modello Numerico per il Calcolo della Struttura," CRS4 Rept., April 2002.

[15]Di Piazza, I., "An Analytical Model of Heat Transfer and Fluid Dynamic Performances of an Unconventional NTR Engine for Manned Interplanetary Missions," CRS4 Rept., May 2004.

[16]Benetti, P., Cinotti, L., Mulas, M., and Stalio, R., "Fission Fragments Direct Heating of Gas Propellant for Space Rocket," *In-Space Propulsion, Book of Proceedings*, IWCP Vol. 10, edited by L. T. DeLuca, R. L. Sackheim, and B. A. Palaszewski, Grafiche GSS, Bergamo, Italy, 2005

[17]Di Piazza, I., Mulas, M., and Varone, A., "Thermo-Fluid Dynamic Analysis of the Fision Fragments Rocket Engine," *Proceedings of UIT Conference*, Italian Union of Thermal-Fluid Dynamics, Udine, Italy, June 2003.